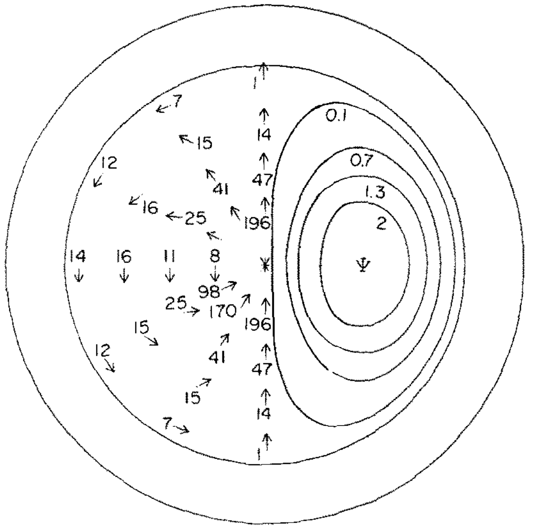


FIG. 4. Dimensionless stream function and velocity at $\tau = 0.1$.

[3]. We take the latter fluid for illustration using the values $\gamma = \lambda = 0.1, \beta = 3, P = 13.4$ and $Ra = 8 \times 10^3$. Results for the sphere are discussed; those for the cylinder are almost identical in structure.

The axisymmetric convective flow rises in the form of a jet along the axis $\theta = \pi$ and $\theta = 0$ to form a forward stagnation point at the north pole $\theta = 0$. It returns downward on both sides of the axis bathing the interface and collides to give a backward stagnation point at $\theta = \pi$. As the liquid volume decreases and looses its sensible heat the density differences increase leading to increased convection. In the early part of the process this form of thermal spin-up initiates the formation of the cusp at the south pole. At the dimensionless time $\tau = 0.4$ the liquid core temperature is below the initial temperature. Thus as the process evolves the liquid temperature will approach the fusion temperature and the circulation will cease.

Interface locations are displayed in Fig. 2 at intervals of $\Delta\tau = 0.1$. The volume of liquid as a function of time is given in Fig. 3; here the dashed curve gives the volume remaining when convection is ignored and such results were found to be in good agreement with the analytical studies of Stewartson and Waechter [1]. Figure 4 displays the streamlines and velocity $av/k$ at $\tau = 0.1$. Detailed results on the temperature distribution and heat transfer coefficients (at the interface and sphere surface) have also been evaluated.

*Acknowledgement*—One of the authors (R.G.) is indebted to SERC for the award of a Research Studentship to support this work.

## REFERENCES


1. K. Stewartson and R. T. Waechter, *Proc. R. Soc.* **A348**, 415–426 (1976).
2. E. M. Sparrow, S. V. Patanker and S. Ramadhyani, *J. Heat Transfer* **99**, 520–526 (1977).
3. E. M. Sparrow, R. R. Schmidt and J. W. Ramsey, *J. Heat Transfer* **100**, 11–16 (1978).
5. C. J. Ho and R. Viskanta, *J. Heat Transfer* **106**, 12–19 (1984).
6. F. M. Chiesa and R. I. L. Guthrie, *J. Heat Transfer* **96**, 377–384 (1974).
7. H. J. Schulze, P. M. Beckett, J. A. Howarth and G. Poots, *Proc. R. Soc.* **A385**, 313–343 (1983).
8. C. J. Ho and R. Viskanta, *Int. J. Heat and Mass Transfer* **27**, 705–715 (1984).
9. H. S. Carslaw and J. C. Jaeger, *Conduction of Heat in Solids*, 2nd edn. Oxford, Clarendon Press (1959).
10. M. Van Dyke, *Perturbation Methods in Fluid Mechanics*. Parabolic Press, Stanford, California (1975).
11. G. Stead, Theoretical aspects of moving interfaces, Ph.D. thesis University of Hull (1976).


*Int. J. Heat Mass Transfer.* Vol. 28, No. 6, pp. 1231–1233, 1985
Printed in Great Britain
0017-9310/85 \$3.00 + 0.00


# Analytical solution for the buoyancy flow during the melting of a vertical semi-infinite region

S. C. HUANG

Mechanical Technology Inc., 968 Albany-Shaker Road, Latham, NY 12110, U.S.A.

(*Received* 29 *November* 1983 *and in final form* 15 *October* 1984)

## NOMENCLATURE

- $g$ acceleration of gravity
- $k$ thermal conductivity
- $p$ pressure
- $Pr$ Prandtl number of the melt, $\nu/\alpha_1$
- $Ste$ Stefan number $k_1(T_0 - T_i)/\rho\alpha_1 L_m$, where $L_m$ = latent heat
- $T_{avg}$ $\frac{1}{2}(T_0 + T_m)$
- $v$ velocity of the melt in the $y$ direction.

Greek symbols
- $\alpha$ thermal diffusivity
- $\beta$ coefficient of thermal expansion, assumed constant
- $\nu$ kinematic viscosity of the melt
- $\rho$ density at $T_{avg}$.

Subscripts
- m at the melting front, $x = X(t)$
- 1 liquid phase
- 2 solid phase
- 21 solid phase divided by liquid phase.

## 1. INTRODUCTION

THE IMPORTANCE of natural convection in the Stefan's problem received attention only in recent years. Both experiments [1] and numerical analyses [2] indicate that the buoyancy-driven flow exists from the onset of the transient process. In addition, the heat transfer mechanism was mainly conduction-controlled for small time and convection-controlled when the critical Grashof number was reached [3]. In spite of these observations, there is not yet a complete analysis of the velocity profile during the early stages of melting. The objective of this note is to report a closed-form solution in a vertical semi-infinite region.

## 2. FORMULATION OF THE PROBLEM

The solid in the region $0 < x < \infty$, $-\infty < y < \infty$ is initially at a uniform temperature $T_i$, where positive $y$ is in the upward direction. The melting process starts from time $t = 0$ as one maintains a constant temperature $T_0(> T_m)$ on the surface $x = 0$. Because of the nonuniform temperature distribution, buoyancy-driven flow is developed in the melt region $0 < x < X(t)$.

During the early stage of the process, the melting speed is conduction-controlled and the problem is one-dimensional. The temperature distribution follows the conventional Neumann's solution and its dimensionless form is [4]

$$\theta_1(\eta) = 1-(1-\theta_m)\frac{\operatorname{erf}(\lambda\eta)}{\operatorname{erf}(\lambda)} \quad 0 < \eta < 1 \tag{1}$$

$$\theta_2(\eta) = \theta_m \frac{\operatorname{erfc}(\lambda\eta/\alpha_{21}^{1/2})}{\operatorname{erfc}(\lambda/\alpha_{21}^{1/2})} \quad 1 < \eta < \infty \tag{2}$$

$$(1-\theta_m)\frac{e^{-\lambda^2}}{\operatorname{erf}(\lambda)} - \frac{k_{21}\theta_m}{\alpha_{21}^{1/2}}\frac{e^{-\lambda^2/\alpha_{21}}}{\operatorname{erfc}(\lambda/\alpha_{21}^{1/2})} = \pi^{1/2}\lambda/Ste \tag{3}$$

where

$$\theta = \frac{T-T_i}{T_0-T_i},\quad \lambda = \frac{X(t)}{2(\alpha_1 t)^{1/2}},\quad \eta = \frac{x}{X(t)}. \tag{4}$$

One assumes here that the density change effect across the phase front is negligible.

The momentum equation of the melt, with the Oberbeck–Boussinesq assumption, takes the following form

$$\frac{\partial v}{\partial t} = -\frac{1}{\rho}\frac{dp}{dy} - \frac{\rho_1}{\rho}g + v\frac{\partial^2 v}{\partial x^2}, \quad 0 < x < X(t), t > 0 \tag{5}$$

where the temperature-dependent density $\rho_1$ corresponds to the driving source of the flow. In general, except water near 4°C, one has

$$\rho_1(T_1) = \rho[1-\beta(T_1(x,t)-T_{avg})]. \tag{6}$$

The initial and the non-slip boundary conditions for $v(x,t)$ are

$$v = 0 \quad \text{for} \begin{cases} t < 0, & 0 < x < \infty \\ x = 0, & t > 0 \\ x = X(t), & t > 0. \end{cases} \tag{7a, 7b, 7c}$$

In addition, the gobal continuity condition for a closed system, i.e. $y = \pm\infty$ are bounded, requires that

$$\int_0^{X(t)} v(x',t)\,dx' = 0, \quad t > 0. \tag{8}$$

## 3. ANALYSIS

Unlike the temperature, the velocity $v(x,t)$ is a function of both time and the similarity variable. One defines a dimensionless velocity $V(\xi)$ as

$$v(x,t) = \frac{\beta g(T_0-T_i)X^2(t)}{v}V(\xi) = 2\beta g(T_0-T_i)\xi_m^2 t V(\xi) \tag{9}$$

where

$$\xi = \xi_m\eta = (2/\mathrm{Pr})^{1/2}\lambda\eta. \tag{10}$$

Accordingly, equations (5)–(7) reduce to

$$\frac{d^2V}{d\xi^2} + \xi\frac{dV}{d\xi} - 2V = -\xi_m^{-2}(\theta_1-\theta_r), \quad 0 < \xi < \xi_m \tag{11}$$

$$V = 0 \quad \text{for} \begin{cases} \xi = 0 & (12a) \\ \xi = \xi_m & (12b) \end{cases}$$

$$\int_0^{\xi_m} V(\xi')\,d\xi' = 0. \tag{13}$$

In the above, $\theta_r = (T_r - T_i)/(T_0 - T_i)$. $T_r$ is a constant reference temperature defined by the pressure gradient parallel to the flow,

$$T_r = T_{avg} + \frac{1}{\beta}\left(1 + \frac{1}{\rho g}\frac{dp}{dy}\right). \tag{14}$$

The appearance of the unknown $\theta_r$ in equation (11) and the unknown velocity $V(\xi)$ in equation (13) makes the direct numerical analysis of equations (11)–(13) very difficult.

The solution of equations (11) and (12) is simply

$$V(\xi) = \xi_m^{-2}\,e^{-\xi^2/4}\int_0^{\xi_m}(\theta_1(\xi')-\theta_r)e^{\xi'^2/4}G(\xi|\xi')\,d\xi'. \tag{15}$$

The Green's function $G(\xi|\xi')$ appearing in equation (15) has the following form

$$G(\xi|\xi') = (\pi/2)^{1/2}\frac{H(\xi',\xi_m)}{H(0,\xi_m)}H(0,\xi)e^{(\xi^2-\xi'^2)/4}, \quad \xi < \xi' \tag{16a}$$

$$= (\pi/2)^{1/2}\frac{H(0,\xi')}{H(0,\xi_m)}H(\xi,\xi_m)e^{(\xi'^2-\xi^2)/4}, \quad \xi' < \xi \tag{16b}$$

where

$$H(a,b) = e^{-(b^2-a^2)/4}[h_3(a)h_4(b)-h_4(a)h_3(b)] \tag{17a}$$

$$h_3(a) = \tfrac{1}{2}e^{-a^2/4}[(\pi/2)^{1/2}(a^2+1)e^{a^2/2}\operatorname{erfc}(a/2^{1/2})-a] \tag{17b}$$

$$h_4(a) = (2/\pi)^{1/2}e^{a^2/4}(a^2+1), \quad a,b = \text{dummy real.} \tag{17c}$$

One may observe that equations (16) and (17) are also valid for water near 4°C, regardless the linear assumption made earlier in equation (6).

In order to obtain the constant $\theta_r$, one first integrates equation (11), with the help of equations (12) and (13), to get

$$\frac{dV(\xi=\xi_m)}{d\xi} - \frac{dV(\xi=0)}{d\xi} = -\xi_m^{-1}\left(\int_0^1 \theta_1(\eta')\,d\eta' + \theta_r\right). \tag{18}$$

Substituting equations (15)–(17) into the above equation and keeping in mind that [5]

$$\frac{\partial H(0,\xi=0)}{\partial\xi} = -\frac{\partial H(\xi=\xi_m,\xi_m)}{\partial\xi} = (2/\pi)^{1/2} \tag{19}$$

are the Wronskians of the parabolic cylinder functions $h_3$ and $h_4$, one gets

$$\theta_r = [\theta_{r\infty} - s_3(\xi_m) + (1-\theta_m)s_4(\lambda,\xi_m)]/[1-s_3(\xi_m)] \tag{20}$$

where

$$\theta_{r\infty} = \theta_m + \frac{(1+\theta_m)(1-e^{-\lambda^2})}{\pi^{1/2}\lambda\operatorname{erf}(\lambda)} \tag{21a}$$

$$s_3(\xi_m) = \frac{(2/\pi)^{1/2}}{H(0,\xi_m)}\left\{[h_3(0)-h_3(\xi_m)e^{\xi_m^2/4}] + \frac{\pi}{4}[h_4(\xi_m)e^{\xi_m^2/4}-h_4(0)]\operatorname{erfc}(\xi_m/2^{1/2})\right\} \tag{21b}$$

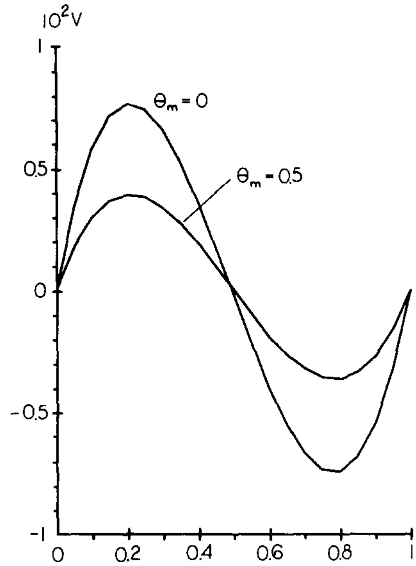


FIG. 1. Dimensionless velocity profiles with $Pr = 0.08$ and $\lambda = 0.2$. For $\theta_m = 0, \theta_r = 0.488$; for $\theta_m = 0.5, \theta_r = (1+0.488)/2 = 0.744$.

$$s_4(\lambda,\xi_m) = \frac{1}{\xi_m H(0,\xi_m)}\int_0^{\xi_m} \frac{\mathrm{erf}(\lambda\xi'/\xi_m)}{\mathrm{erf}(\lambda)} \times [e^{-(\xi_m^2-\xi'^2)/2} H(0,\xi') + H(\xi',\xi_m)]\,d\xi'. \quad (21c)$$

It is easy to show that $s_3(\infty) = s_4(\lambda,\infty) = 0$ and consequently $\theta_r = \theta_{r\infty}$ when $\xi_m \to \infty$. For the case where $\xi_m \to 0$, one can solve equations (11)–(13) directly to yield

$$V(\eta) = \frac{1-\theta_r}{2}\eta(1-\eta) - \frac{1-\theta_m}{2\lambda}\left[\left(\frac{1+2\lambda^2}{2\lambda} + \frac{e-\lambda^2}{\pi^{1/2}\mathrm{erf}(\lambda)}\right)\eta - \frac{1+2\lambda^2\eta^2}{2\lambda}\frac{\mathrm{erf}(\lambda\eta)}{\mathrm{erf}(\lambda)} - \frac{\eta}{\pi^{1/2}}\frac{e^{-\lambda^2\eta^2}}{\mathrm{erf}(\lambda)}\right] \quad (22)$$

in which

$$\theta_r = \tfrac{1}{2}(1+\theta_m) - \tfrac{1}{2}(1-\theta_m)\left[1 - \frac{3}{\lambda^2} + \frac{2e^{-\lambda^2}}{\pi^{1/2}\lambda\,\mathrm{erf}(\lambda)} + \frac{4(1-e^{-\lambda^2})}{\pi^{1/2}\lambda^3\,\mathrm{erf}(\lambda)}\right]. \quad (23)$$

However, this latter limiting case corresponds only to a trivial dimensional velocity.

## 4. RESULTS AND DISCUSSION

The obtained closed-form solution is numerically straightforward. The relevant parameters are $Pr$, $\lambda$ and $\theta_m$. To illustrate, one takes $Pr = 0.08$ and $\lambda = 0.2$. The small Prandtl number chosen here may correspond to an early development of strong buoyancy flow, as is indicated by equation (9).

Figure 1 shows the dimensionless velocity profiles $V(\eta)$ for two cases, $\theta_m = 0$ and $\theta_m = 0.5$. Since the melt has higher temperature close to the wall, $x = 0$, the flow is upward in the warm region and downward in the cold region as expected. The reversal of the flow direction occurs slightly before the midpoint $\eta = 0.5$. In addition, the upward flow has slightly greater maximum velocity than the downward flow. This means that the shear stress at the wall is greater than that at the interface. Since $\theta_m = 0.5$ corresponds to a smaller temperature difference in the melt, its $V(\eta)$ profile in Fig. 1 is about half the size of that for $\theta_m = 0$.

One may use the above results in stability analysis to determine the onset of convection-controlled melting.

## REFERENCES


1. G. S. Cole, Temperature measurement and fluid flow distributions ahead of solid–liquid interface, *Trans. Am. Inst. mech. Engrs* **239**, 1287–1295 (1967).
2. E. M. Sparrow, S. V. Patankar and S. Ramadhyani, Analysis of melting in the presence of natural convection in the melt region, *Trans. Am. Soc. mech. Engrs*, Series C, *J. Heat Transfer* **99**, 520–526 (1977).
3. M. A. Hassab and M. M. Sorour, Onset of convection in a melted ice layer between vertical plates, *Int. J. Heat Mass Transfer* **25**, 909–916 (1982).
4. H. S. Carslaw and J. C. Jaeger, *Heat Conduction in Solids.* Oxford University Press, London (1959).
5. M. Abramowitz and I. A. Stegun, *Handbook of Mathematical Functions.* National Bureau of Standards Appl. Math. Ser. No. 55 (1972).